Eur. Phys. J. C 22, 493–501 (2001)
Digital Object Identifier (DOI) 10.1007/s100520100823

THE EUROPEAN PHYSICAL JOURNAL C

Modified Breit–Wigner formula for mesonic resonances describing OZI decays of confined $q\bar{q}$ states and the light scalar mesons

E. van Beveren[1,a], G. Rupp[2,b]

[1] Centro de Física Teórica, Departamento de Física, Universidade de Coimbra, 3000 Coimbra, Portugal
[2] Centro de Física das Interacções Fundamentais, Instituto Superior Técnico, Edifício Ciência, 1049-001 Lisboa Codex, Portugal

Received: 15 October 2001 /
Published online: 21 November 2001 –

Abstract. A general expression resembling the Breit–Wigner formula is derived for the description of resonances which appear in meson–meson scattering. Our starting point is a unitarised meson model, but reduced to a simpler form and freed from the specific assumption about the confining force. The parameters of the resulting "resonance-spectrum expansion" are directly related to the confinement spectrum and the mechanism of $^3P_0$ valence-quark-pair creation for OZI-allowed hadronic decay, and not to the central positions and widths of resonances. This method also provides us with a straightforward explanation for the origin of the light scalar mesons without requiring extra degrees of freedom.

1 Introduction

Lattice QCD in principle offers the most direct way to link to experiment what we believe to be the fundamental theory of the strong interactions. However, for the time being only quenched calculations are capable of making, with a reasonable accuracy, predictions for e.g. the masses of the mesons, as a result of the confinement sector of QCD [1–4]. Relating such predictions to experimental data is quite a controversial issue though, since the states obtained in quenched lattice QCD (qlQCD) are manifestly stable, a circumstance which clearly does not occur in experiment, at least for most mesons. The reason of course is the difficulty of incorporating quark-pair creation in qlQCD, thus impeding the process of OZI-allowed strong decay, which is responsible for the large widths of many mesonic resonances. But also the central positions of such resonances may be quite displaced due to the effects of strong decays [5], when compared with the stable qlQCD states. Moreover, the contributions of *virtual hadronic* decays through quark loops owing to the presence of *closed OZI-allowed* thresholds, which should also lead to real mass shifts, are not fully accounted for in qlQCD [6–8]. An additional complication is the observation that not even the *number of* $q\bar{q}$ states in the $J^P = 0^+$ sector of the qlQCD predictions seems to agree with experiment [9], thus contributing to the general confusion concerning especially the light scalar mesons.

It is evidently a very unsatisfactory state of affairs that, notwithstanding the ever improving accuracy of the numerical predictions in qlQCD, these cannot be trusted to unmistakably confirm possible signals of new physics. In the present paper, we shall propose an alternative method of data analysis, which does allow for an accurate link between qlQCD, or any other, model-dependent formulation of confinement, and experiment. In the process we are also going to find a reliable approach to the light scalar mesons ($< 1\,\mathrm{GeV}$).

The idea is simple and amounts to the observation that valence-quark-pair creation connects the states of qlQCD to the resonances which in experiment are seen in elastic and inelastic meson–meson cross sections. Hence, if we model quark-pair creation in such a way that it theoretically can be turned on and off, then we are capable to predict the qlQCD states in the model limit of no-quark-pair creation. Such a philosophy already underlay an elaborate coupled-channel quark model [10–13], designed to simultaneously describe mesonic bound-state spectra, resonances, and meson–meson scattering. However, in spite of the model's success to reproduce a host of experimental data with a very limited number of parameters, it is clearly not suited as a tool for data analysis, owing to the specific model choice of the confining $q\bar{q}$ potential, and furthermore the rather complicated matrix expressions needed to obtain S-matrix-related observables. Therefore, in this work our strategy will be the following. By replacing the specific confinement part of the Hamiltonian of [10–13] by a more general one, we allow here for any arbitrary discrete spectrum of "bare" $q\bar{q}$ states. At the same time, by

[a] e-mail: eef@teor.fis.uc.pt
[b] e-mail: george@ajax.ist.utl.pt

using a simpler form for the coupling potential, describing the transitions between the $q\bar{q}$ and meson–meson sectors through $^3P_0$ quark-pair creation, the complexity of the model's scattering solutions is substantially reduced. The resulting exact, closed-form formula for the S-matrix is subsequently fitted to the experimental data, i.e., partial-wave cross sections or phase shifts for meson–meson scattering, by adjusting the model parameters. Afterwards, we may study the theoretical limit of vanishing valence-quark-pair creation, described by a sole parameter, which decouples the bare states from the meson–meson continuum. The latter are supposed to be equivalent to the states found in qlQCD. Consequently, the masses of the thus resulting spectrum could then be compared with those from qlQCD calculations.

The organisation of the present paper is as follows. In Sect. 2 we develop a model-independent partial-wave S-matrix for the description of elastic and inelastic two-meson scattering. A so-called "resonance-spectrum expansion" (RSE) is discussed in section (2.2). In Sect. 3 the RSE is compared to the data for elastic $K\pi$ S-wave phase shifts and P-wave cross sections in the one-threshold limit. The complex singularities of the corresponding S-matrices are shown to allow for an easy relation to the $q\bar{q}$ confinement spectrum. The conclusions are presented in Sect. 4.

2 Breit–Wigner-like scattering amplitudes

A suitable model in which the communication between the confinement sector of strong interactions with the two-meson continuum is enabled through valence-quark-pair creation has been proposed in a series of articles [10–13]. It allows for the determination of partial-wave two-meson elastic and inelastic scattering cross sections, as well as for the search of singularities in the partial-wave coupled-channel two-meson scattering matrix for all possible valence flavours. Hence, it enables the calculation of resonances above and bound states below the lowest threshold, i.e., the meson spectrum. In the limit of no valence-quark-pair creation one obtains the confinement spectrum, or bare states, which may be compared to the states of qlQCD. The model has four parameters and four constituent quark masses. No distinction is made between up and down quarks. One of the model parameters parametrises the employed confinement mechanism (harmonic oscillator), whereas the other three parametrise the communication between the two distinct sectors of the model, that is, the permanently closed confinement channels and the meson–meson continuum channels. The model yields, with one set of four parameters and one set of four constituent quark masses, good results for heavy quarkonia [13] and light-meson spectra [11], including the scalars [10], as well as for two-meson scattering data [10, 11].

Let us first study the generic form of the scattering matrix for permanently closed channels coupled to several meson–meson scattering channels, in a simplified version of the above model.

2.1 Scattering matrix for several coupled channels

When we describe quarkonia by wave functions $\psi_{\rm c}$ and two-meson systems by wave functions $\psi_{\rm f}$, then we obtain for their time evolution the wave equations

$$(E - H_{\rm c})\,\psi_{\rm c}\,(\boldsymbol{r}) = V_t\psi_{\rm f}\,(\boldsymbol{r})$$

and

$$(E - H_{\rm f})\,\psi_{\rm f}\,(\boldsymbol{r}) = [V_t]^{\rm T}\,\psi_{\rm c}\,(\boldsymbol{r})\,. \tag{1}$$

Here, $H_{\rm c}$ describes the dynamics of confinement in the interaction region, $H_{\rm f}$ the dynamics of the scattered particles, and V_t the communication between the two different sectors.

For the dynamics of confinement we understand here that, as a function of the interquark distance r, the resulting quark–antiquark binding forces grow rapidly outside the interaction region. Consequently, we must eliminate $\psi_{\rm c}$ from (1), since it is vanishing at large distances and thus *unobservable*. Formally, this is easy to do. We then obtain the relation

$$(E - H_{\rm f})\,\psi_{\rm f}\,(\boldsymbol{r}) = [V_t]^{\rm T}\,(E - H_{\rm c})^{-1}\,V_t\psi_{\rm f}\,(\boldsymbol{r})\,. \tag{2}$$

By comparison of (2) with the usual expressions for the scattering wave equations, we must conclude that the generalised potential V, which results from the set of coupled equations (1), is here given by

$$V = [V_t]^{\rm T}\,(E - H_{\rm c})^{-1}\,V_t. \tag{3}$$

In the momentum representation (3) takes the form

$$\langle\boldsymbol{p}|V|\boldsymbol{p}'\rangle = \langle\boldsymbol{p}|\,[V_t]^{\rm T}\,(E - H_{\rm c})^{-1}\,V_t|\boldsymbol{p}'\rangle. \tag{4}$$

Let us denote the configuration-space representation of the properly normalised eigensolutions of the operator $H_{\rm c}$ of (1), corresponding to the energy eigenvalue $E_{n\ell_{\rm c}}$, by

$$\langle\boldsymbol{r}\,|n\ell_{\rm c}m\rangle = Y_m^{(\ell_{\rm c})}\,(\hat{r})\,\mathcal{F}_{n\ell_{\rm c}}\,(r)\,,$$
$$\text{where}\begin{cases} n = 0, 1, 2, \ldots, \\ \ell_{\rm c} = 0, 1, 2, \ldots, \\ m = -\ell_{\rm c}, \ldots, +\ell_{\rm c}. \end{cases} \tag{5}$$

Here, n and $\ell_{\rm c}$ represent the orbital radial and angular excitations of the quark–antiquark system, respectively. Hence, when we let the self-adjoint operator $H_{\rm c}$ act to the left, we obtain for (4) the expression

$$\begin{aligned}\langle\boldsymbol{p}|V|\boldsymbol{p}'\rangle &= \sum_{n\ell_{\rm c}m}\langle\boldsymbol{p}|\,[V_t]^{\rm T}\,|n\ell_{\rm c}m\rangle\langle n\ell_{\rm c}m|\,(E - H_{\rm c})^{-1}\,V_t|\boldsymbol{p}'\rangle \\ &= \sum_{n\ell_{\rm c}m}\langle\boldsymbol{p}|\,[V_t]^{\rm T}\,\frac{|n\ell_{\rm c}m\rangle\langle n\ell_{\rm c}m|}{E - E_{n\ell_{\rm c}}}V_t|\boldsymbol{p}'\rangle.\end{aligned} \tag{6}$$

Evaluation of this equation leads to the Born term of the transition amplitude.

However, now we find it opportune to select the operators $H_{\rm f}$ and V_t such that it becomes possible to determine all higher-order terms of the transition amplitude.

By doing so, we leave no doubt about the analyticity and unitarity properties of the resulting scattering matrix. In configuration space we define these operators by

$$H_{\rm f} = -\frac{1}{2}\mu^{-1}\nabla_r^2 + M_1 + M_2$$

and

$$V_t = \frac{\lambda}{a^{3/2}}\bar{V}_t\delta\left(r-a\right), \tag{7}$$

where μ represents the reduced-mass matrix of the meson–meson system, and $M_{1,2}$ stand for matrices that contain the masses of the two mesons in each scattering channel. We limit ourselves to diagonal mass matrices in this work.

The transition potential V_t in (7) is, as we shall see below, a reasonable approximation to the quark-pair-creation transition potentials described in [14]. It is parametrised by λ, which determines its intensity, and by a, which stands for the average distance between the interacting particles (either a quark and an antiquark, or two mesons) where transitions from one sector to the other take place. In practice, a should come out of the order of 1 fm, which is confirmed by adjusting the model parameters to the experimental data. $\bar{V}_t$ is the matrix that contains the relative intensities for transitions between the meson–meson and quark–antiquark sector(s). Notice that we assume here spherical symmetry for all interactions.

With the choices of (7), we obtain for the full (to all orders in λ) partial-wave scattering matrix the exact expression

$$\begin{aligned} S_\ell\left(E\right) = &\left[1-2{\rm i}\frac{\lambda^2}{a}p^{-1/2}H^{(2)}(a)\mu^{1/2}\left[\bar{V}_t\right]^T\right. \\ &\left.\times\sum_{n=0}^{\infty}\frac{\left|\mathcal{F}_{n\ell_{\rm c}}(a)\right|^2}{E-E_{n\ell_{\rm c}}}\bar{V}_t\mu^{1/2}J(a)p^{-1/2}\right] \\ &\times\left[1+2{\rm i}\frac{\lambda^2}{a}p^{-1/2}H^{(1)}(a)\mu^{1/2}\left[\bar{V}_t\right]^{\rm T}\right. \\ &\left.\times\sum_{n=0}^{\infty}\frac{\left|\mathcal{F}_{n\ell_{\rm c}}(a)\right|^2}{E-E_{n\ell_{\rm c}}}\bar{V}_t\mu^{1/2}J(a)p^{-1/2}\right]^{-1}, \end{aligned} \tag{8}$$

where p, μ, $J(a)$ and $H^{(1,2)}(a)$ are diagonal matrices throughout this work, with as many diagonal elements as meson–meson channels considered. The non-vanishing matrix element

$$p_i = [p]_{ii} \tag{9}$$

represents the relative linear momentum in the centre-of-mass (CM) system of the ith scattering channel. The diagonal elements of $J(a)$ and $H^{(1,2)}(a)$ are related to the usual spherical Bessel and Hankel functions by

$$[J(a)]_{ii} = p_i a j_{\ell_i}\left(p_i a\right)$$

and

$$\left[H^{(1,2)}(a)\right]_{ii} = p_i a h^{(1,2)}_{\ell_i}\left(p_i a\right), \tag{10}$$

where ℓ_i stands for the relative angular momentum in the ith scattering channel.

The matrix $\bar{V}_t$ contains the coupling constants which are worked out in [15]. In case only one $q\bar{q}$ channel is considered (S-wave meson–meson scattering for isodoublet and isovector), the matrix $\bar{V}_t$ is just a row vector. Then the expression

$$\sum_{n=0}^{\infty}\frac{\left|\mathcal{F}_{n\ell_{\rm c}}(a)\right|^2}{E-E_{n\ell_{\rm c}}} \tag{11}$$

is just a real number, that is, a function of the total CM energy E.

In case one considers more $q\bar{q}$ channels (S-wave meson–meson scattering for isoscalar coupled $n\bar{n}$ and $s\bar{s}$ channels, or P- and higher-wave scattering), $\bar{V}_t$ has as many rows as $q\bar{q}$ channels. Then the resonance sum (11) is a real matrix of the size of the number of $q\bar{q}$ channels.

2.2 The resonance-spectrum expansion

Expression (8) contains very little model dependence. It combines simple kinematics with the experimental observation that resonances occur in non-exotic scattering processes of mesons. Not even assumptions are made about possible final-state interactions, which is expressed by the choice for $H_{\rm f}$ in (7). Consequently, since it is not contaminated with model-dependent prejudices, expression (8) is extremely suitable for the analysis of experimental results in two-meson scattering. Precise determination of the experimental values for $E_{n\ell_{\rm c}}$ and $\left|\mathcal{F}_{n\ell_{\rm c}}(a)\right|^2$ in the resonance sum (11) will give support to the study of the confinement dynamics and the mechanism of hadronic decay. Below we shall show how well the procedure works for data analysis.

In [10,11,13] all possible pseudoscalar–pseudoscalar, pseudoscalar–vector, and vector–vector scattering channels are coupled, through $^3P_0$ non-strange and strange quark-pair creation, to the relevant valence quark–antiquark channels. For isovector and isodoublet flavours one then has one (for S-wave scattering) or two (for P- and higher-waves) permanently closed channels coupled to many scattering channels. For the light isoscalars the number of permanently closed channels is doubled, one channel for $n\bar{n}$ and one for $s\bar{s}$. The intensities of the relative couplings for the transitions between permanently closed channels and the various scattering channels are controlled by flavour independence, which is an observed property of the strong interactions [16]. This has been worked out in [17], and in some more detail in [15,18]. As a result, also in [10,11,13] only one overall parameter is left for all possible transition intensities, which can be switched on and off. The behaviour of this more complex model is, especially near the lowest threshold, very similar to the behaviour of the scattering matrix given in formula (8).

In [10,11,13], a harmonic oscillator with flavour-independent frequency was chosen for the description of the confinement dynamics in the permanently closed channels. Hence, by switching off the overall transition parameter, one obtains the harmonic-oscillator spectrum.

On the other hand, by switching it on, the experimental data for two-meson scattering are reproduced, as well as bound states like the kaon and the J/Ψ. Here, we do not intend to specify the confinement Hamiltonian $H_{\rm c}$ of (1), but shall follow a different strategy. We observe that the expressions $\mathcal{F}_{n\ell_{\rm c}}(a)$ in formula (8), i.e., the values of the eigenfunctions of the confinement operator $H_{\rm c}$ at distance a, are c-numbers independent of the total CM energy E. In the model of [10,11], $\mathcal{F}_{n\ell_{\rm c}}(a)$ and $E_{n\ell_{\rm c}}$ represent the harmonic-oscillator eigenstates and eigenvalues, respectively, which need only one free parameter, the oscillator frequency. However, since the confinement mechanism is here supposed to be unknown, we might as well substitute $|\mathcal{F}_{n\ell_{\rm c}}(a)|^2$ and $E_{n\ell_{\rm c}}$ by arbitrary non-negative real constants, $B_{n\ell_{\rm c}}$ and $E_{n\ell_{\rm c}}$, to be adjusted to the experimental data, i.e.,

$$\sum_{n=0}^{\infty}\frac{|\mathcal{F}_{n\ell_{\rm c}}(a)|^2}{E-E_{n\ell_{\rm c}}}=\sum_{n=0}^{\infty}\frac{B_{n\ell_{\rm c}}}{E-E_{n\ell_{\rm c}}}. \tag{12}$$

In practical calculations, one may limit the sum in this "resonance-spectrum expansion" (RSE) to a few ($=N$) resonances only, and approximate the sum of the remaining terms by a constant, assuming $E\ll E_{n\ell_{\rm c}}$ for $n>N$. This way one obtains Breit–Wigner-like expressions.

By redefining λ and the $B_{n\ell_{\rm c}}$'s one might take the above-referred constant equal to -1, according to

$$\lambda^2\sum_{n=0}^{\infty}\frac{B_{n\ell_{\rm c}}}{E-E_{n\ell_{\rm c}}}\to\lambda^2\left\{\sum_{n=0}^{N}\frac{B_{n\ell_{\rm c}}}{E-E_{n\ell_{\rm c}}}-1\right\}. \tag{13}$$

An alternative approach is to absorb λ^2 into the $B_{n\ell_{\rm c}}$'s and then separate the relevant terms and the remaining sum. We shall not follow this strategy, since we want to keep explicit the dependence on the parameter which provides the communication between the scattering and confinement sectors.

At this point it is opportune to discuss the model dependence of our procedure. By the substitution (12), any relation to the quantum numbers of the confinement sector is lost. We just continue to label the $B_{n\ell_{\rm c}}$'s and $E_{n\ell_{\rm c}}$'s in order to distinguish them properly. It also implies that a direct reference to the $^3P_0$ mechanism is lost. What is left is just the choice (7) for the remaining operators, where $H_{\rm f}$ does not even contain final-state interactions, and V_t is a spherically symmetric local approximation to almost any possible transition mechanism that provides the experimentally observed OZI-allowed communication between the confinement and meson–meson scattering sectors. In summary, the model only assumes that non-exotic meson–meson scattering is dominated by the coupling to s-channel resonances.

3 One threshold

Let us consider the case of one permanently closed channel coupled to one meson–meson scattering channel. Using formulae (8) and (12), one deduces the partial-wave scattering phase shift $\delta_\ell(p)$ for elastic meson–meson scattering, which is a function of the relative momentum in the CM frame,

$$\mathrm{cotg}\,(\delta_\ell(p))=\frac{n_\ell(pa)}{j_\ell(pa)}-\left[2\lambda^2\mu pa j_\ell^2(pa)\sum_{n=0}^{\infty}\frac{B_{n\ell_{\rm c}}}{E-E_{n\ell_{\rm c}}}\right]^{-1}, \tag{14}$$

with $\bar{V}_t$ absorbed in λ.

Notice that the partial-wave phase shifts vanish for $\lambda\to 0$, unless one takes at the same time the limit $E\to E_{n\ell_{\rm c}}$, which represents therefore the no-interaction limit in the two-meson system. It is indeed the parameter λ that switches valence-quark-pair creation on and off.

Formula (14) has similar features as standard Breit–Wigner approximations [19–26] for resonant phenomena. However, from the values of $E_{n\ell_{\rm c}}$ and $B_{n\ell_{\rm c}}$, one cannot read off the positions of the singularities. At most, one might determine an approximate formula which is good for small values of λ, namely

$$E_{n\ell_{\rm c}}-B_{n\ell_{\rm c}}\left[\sum_{n'\neq n}\frac{B_{n'\ell_{\rm c}}}{E_{n\ell_{\rm c}}-E_{n'\ell_{\rm c}}}-\frac{\mathrm{i}}{2\lambda^2\mu pa j_\ell(pa)h_\ell^{(1)}(pa)}\right]^{-1}, \tag{15}$$

concerning singularities in the complex energy plane. Their precise locations can be determined numerically, starting from the approximate values (15).

The values of $E_{n\ell_{\rm c}}$ correspond to the confinement spectrum. These are the quantities of interest in this work. Let us consider next the case of $K\pi$ scattering, as an example.

3.1 $K\pi$ P-wave scattering

Since the pion is a rather light particle, we prefer to employ relativistic kinematics for the relation between the relative linear momentum p in the $K\pi$ system and the total CM energy E, i.e.,

$$E=\sqrt{p^2+m_\pi^2}+\sqrt{p^2+m_K^2} \tag{16}$$

or

$$p=\frac{E}{2}\left[\left\{1-\left(\frac{m_\pi+m_K}{E}\right)^2\right\}\left\{1-\left(\frac{m_\pi-m_K}{E}\right)^2\right\}\right]^{1/2}.$$

Correspondingly, for the reduced mass of the $K\pi$ system we define

$$\mu(E)=\frac{1}{2}\frac{\mathrm{d}p^2}{\mathrm{d}E}=\frac{E}{4}\left[1-\left(\frac{m_K^2-m_\pi^2}{E^2}\right)^2\right]. \tag{17}$$

In Fig. 1 we show the result of formula (14) for the cross sections of $I=1/2$ elastic P-wave scattering, for the

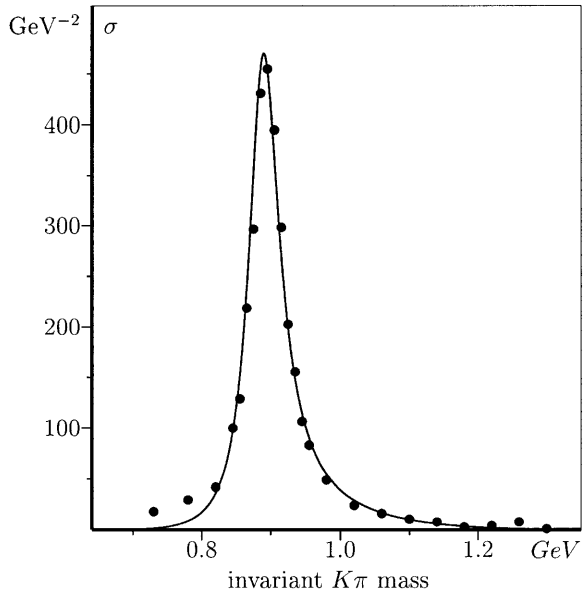

Fig. 1. Comparison of formula (14) and substitution (18) with the experimental cross sections for kaon–pion $I = 1/2$ P-wave scattering. The data are taken from [27]

parameter values $\lambda = 0.75\,\mathrm{GeV}^{-3/2}$ and $a = 5\,\mathrm{GeV}^{-1}$, and with the substitution

$$\sum_{n=0}^{\infty} \frac{B_{n,0}}{E - E_{n,0}} \longrightarrow \frac{0.5}{E - 0.945} - 1\,\mathrm{GeV}^2, \qquad (18)$$

where we neglect possible $\ell_c = 2$ contributions.

The theoretical curve agrees well with the data. For the P-wave $K\pi$ scattering length, we find here the somewhat too low result $a_1^{1/2} = 0.0085\,m_\pi^{-1}$, to be compared to the experimental values taken from [28] (in units of m_π^{-1}), namely 0.017 [29], 0.018 ± 0.002 [30], and 0.018 [31], or to the chiral-perturbation theory result 0.013 ± 0.003 [32]. Nevertheless, the procedure of the substitution (18) leads to a more than satisfactory description in the relevant domain of CM energy, thus allowing one to read off the value for the bare $K^*(892)$ mass, i.e., 0.945 GeV.

Moreover, one may inspect the scattering matrix, which follows from expression (14) after substitution (18), for its singularities in the complex energy plane. One finds one pole at

$$0.887 - 0.027\mathrm{i}\,\mathrm{GeV}. \qquad (19)$$

The relation between the position of the singularity and the Breit–Wigner-like parameters is lost. However, one gains a simple relation to the confinement spectrum. Moreover, in the substitution (18) one may take an arbitrary number of resonances into account.

In order to verify that singularity (19) stems from the bare state at 945 MeV, we may stepwise switch off the model parameter λ and inspect the theoretical positions of the corresponding singularities. This procedure is shown in Fig. 2.

It demonstrates beyond any doubt the relation between the singularity (19) and the bare state at 945 MeV.

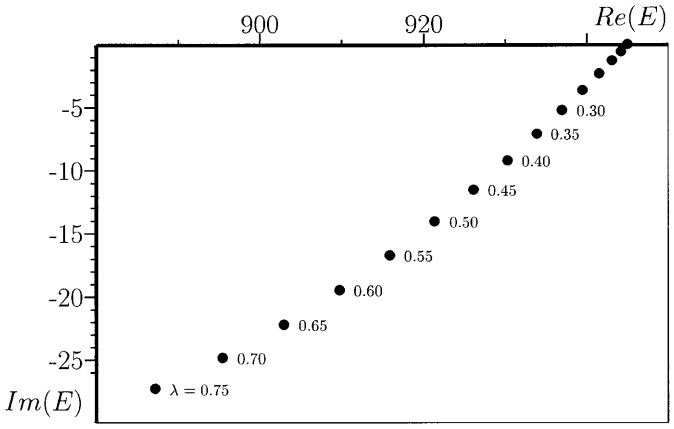

Fig. 2. Complex energy pole positions of the scattering matrix, which result from formula (14) and substitution (18), as a function of the coupling constant λ. The point on the real axis corresponds to the bare state ($\lambda = 0$). Units are in MeV

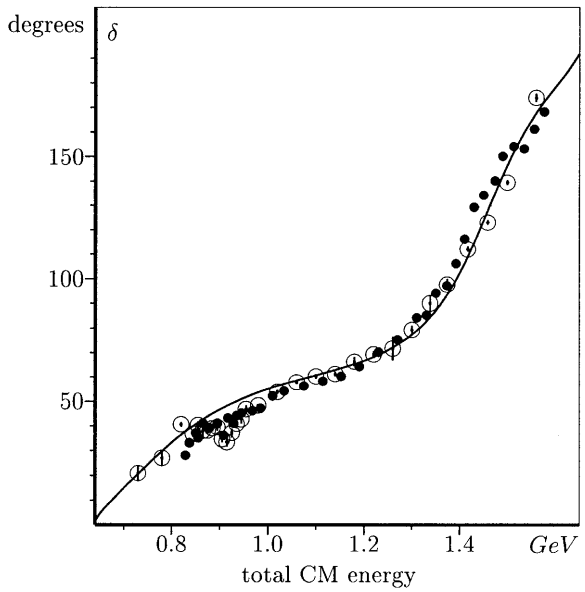

Fig. 3. Comparison of formula (14) and substitution (20) with the experimental phase shifts for kaon–pion $I = 1/2$ S-wave scattering. The data are taken from [27,33] ($\odot$) and [34] ($\bullet$)

Notice that the *motion* of the singularity for small values of λ is perturbative and quadratic in λ, as indicated by expression (15). However, for larger values of the coupling constant the singularity positions become more and more non-perturbative.

3.2 $K\pi$ S-wave scattering

In Fig. 3 we show the result of formula (14) for the phase shifts of $I = 1/2$ elastic S-wave scattering, for the values $\lambda = 0.75\,\mathrm{GeV}^{-3/2}$ and $a = 3.2\,\mathrm{GeV}^{-1}$, and with the substitution

$$\sum_{n=0}^{\infty} \frac{B_{n,1}}{E - E_{n,1}} \longrightarrow \frac{1.0}{E - 1.31} + \frac{0.2}{E - 1.69} - 1\,\mathrm{GeV}^2. \quad (20)$$

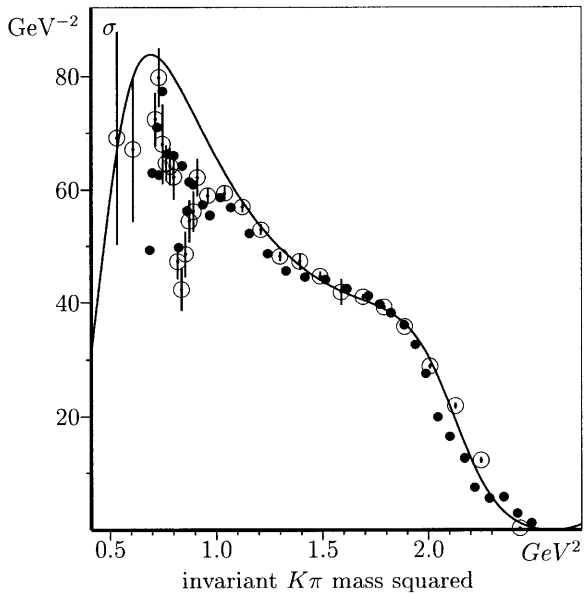

Fig. 4. Kaon–pion $I = 1/2$ S-wave cross sections deduced from the phase shifts of Fig. 3

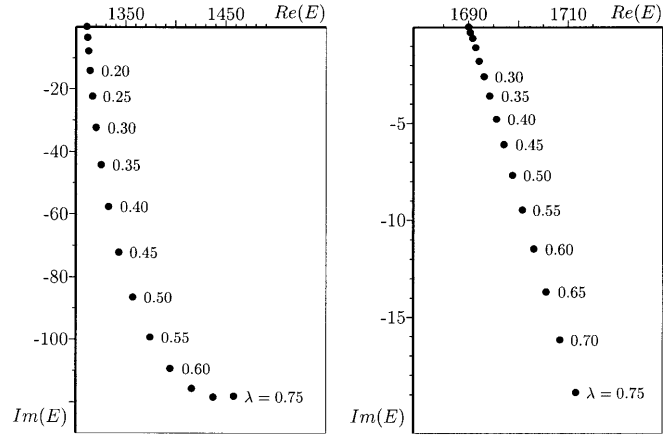

Fig. 5. Complex energy pole positions of the scattering matrix, which result from formula (14) and substitution (20), as a function of the coupling constant λ. The points on the real axes correspond to the bare states ($\lambda = 0$). Units are in MeV

Also for S-wave scattering we find good agreement between the theoretical curve and the data. The difference between P- and S-wave for the radius a of the transition potential agrees well with the corresponding difference for the full pseudoscalar–pseudoscalar transition potentials depicted in Figs. 7 and 8 of [14], respectively. For the S-wave $K\pi$ scattering length we find here $a_0^{1/2} = 0.22\, m_\pi^{-1}$, to be compared to the experimental values taken from [28] (in units of m_π^{-1}), i.e., 0.33 ± 0.01 [27], 0.237 [29], 0.240 ± 0.002 [30], 0.13 ± 0.09 [31], and 0.22 ± 0.04 [35], or to the chiral-perturbation theory result 0.17 ± 0.02 [32].

From (20) one reads for the lowest $J^P = 0^+$ isodoublet eigenstates of confinement the bare masses

$$E_{0,1} = 1.31\,\text{GeV}$$

and

$$E_{1,1} = 1.69\,\text{GeV}. \tag{21}$$

However, when we search in formula (14), after substitution (20), for singularities, then we find besides the two corresponding singularities at

$$(1.458 - 0.118\text{i})\,\text{GeV}$$

and

$$(1.713 - 0.019\text{i})\,\text{GeV} \tag{22}$$

also an additional one at

$$(0.714 - 0.228\text{i})\,\text{GeV}. \tag{23}$$

In Fig. 4 we depict the transformation of the theoretical and experimental phase shifts of Fig. 3 into the $I = 1/2$ elastic partial S-wave cross sections, which show a clear signal at about 830 MeV, with a width of some 500 MeV, as possibly also seen in a very recent experiment by the E791 collaboration [36]. Notice, however, that neither the theoretical, nor the experimental cross sections exhibit a dip, characteristic for Breit–Wigner distributions.

The singularity (23), which in model [10] comes out at $(0.727 - 0.263\text{i})$ GeV, is interpreted as the isodoublet partner $K_0^*(727)$ of the $f_0(400\text{–}1200)$. A corresponding resonance has also been reported in several other works [37–50] in more recent years. The preliminary experimental result of the E791 collaboration reported in [36] awaits further confirmation.

The singularities (22) correspond to the ground state ($n = 0$, $\ell_c = 1$) at $E_{0,1}$ and the first radially excited state ($n = 1$, $\ell_c = 1$) at $E_{1,1}$ of the confinement spectrum, respectively. By reducing the value of the coupling constant λ, the singularities (22) move towards $E_{0,1}$ and $E_{1,1}$, respectively, which can be most clearly understood from expression (15). The complex energy singularities of the partial S-wave scattering matrix (8), resulting from stepwise reducing the theoretical coupling constant λ in formula (14), are depicted in Fig. 5.

It clearly demonstrates the relation between the singularities (22) and the bare states (21). Non-perturbative effects for larger values of the coupling constant can in particular be observed for the lower of the two resonances. First- (or second-) order perturbative calculations would result in completely different positions for the singularities corresponding to the model value of the coupling constant. Especially the real part of the *mass shift* is strongly affected by higher-order corrections. In a recent K-matrix analysis [51], as well as in a covariant quarkonium model [52], it is indeed also found that the bare state might be appreciably lower than the central resonance position for the $K_0^*(1430)$.

The $K_0^*(727)$ singularity (23) does not have a direct relation to any of the states stemming from the confinement mechanism. This fact is also most clearly demonstrated by

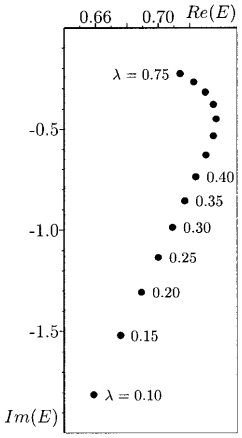

Fig. 6. Complex energy pole positions of the scattering matrix, which result from formula (14) and substitution (20), as a function of the coupling constant λ. Units are in GeV

the theoretical process of decoupling the πK sector from the strange–non-strange quarkonium sector, as depicted in Fig. 6.

The singularity (23) acquires a larger imaginary part when λ is reduced, thus describing a state with ever increasing width, which is a highly non-perturbative phenomenon. For vanishing coupling constant, one observes that the $K_0^*(727)$ disappears into the scattering background. This is a very important observation, since it implies that the $K_0^*(727)$ singularity is a consequence of the transition mechanism that provides the communication between the πK sector and the strange–non-strange quarkonium sector. No such phenomena are observed for P- and higher-wave meson–meson scattering. So we may conclude that a corresponding effect is screened from observation by the centrifugal barrier in (2). Consequently, the mechanism of valence-quark-pair creation appears to be more important in S-wave meson–meson scattering.

The absence of a direct relation between the $K_0^*(727)$ singularity and the non-strange–strange quarkonium sector has for the first time been demonstrated in [10], where similar singularities are shown to describe the properties of the $f_0(400–1200)$, $f_0(980)$, and $a_0(980)$ resonances, thereby resolving two important issues: the nature of the light scalar mesons and the completion of the light scalar nonet.

The positions of the various singularities for πK S-wave scattering in the complex energy plane as a function of λ can of course be obtained from the analyticity properties of the scattering matrix $S(E)$ (8), or, as no approximations are made in the determination of $S(E)$, directly from the dynamical equations (1) and (7). In an extensive study on multichannel scattering with permanently closed channels [53], resonances like the one here described, $K_0^*(727)$, are distinguished from the *fundamental* resonances related to the bound states of H_c, and referred to as *hadron molecular states*. The idea of *meson molecules* has been worked out in several papers [54,55], as a possible explanation for the light scalar mesons $a_0(980)$ and $f_0(980)$. However, the term *molecule* gives the wrong impression that the $q\bar{q}$ component has no importance for these states. From the dynamical equations (1) one may determine the contribution of the strange–non-strange quarkonium sector to the wave functions for any of the states under the $K_0^*(727)$ resonance.

The theoretical distribution of Fig. 4 could well be used for experimental analysis, by optimising the adjustment of the parameters here proposed to the data. Especially the absence of the dip in the cross section is well accounted for in formula (14) with substitution (20). It has moreover the advantage that a direct relation exists between the theoretical distribution and the phase shifts and scattering matrices, which enables the precise location of the singularity associated with the $K_0^*(727)$.

4 Conclusions

We have shown that the RSE parameters $E_{n\ell_c}$ of formula (12) relate experiment to qlQCD calculations of hadron masses better than the usual central Breit–Wigner positions of resonances do. This is not only a consequence of the potentially large mass shifts due to hadronic decay, but also is due to the nice feature of the RSE procedure that S-matrix singularities not originating from genuine confinement can easily be isolated. As an important application of the RSE, it is shown here, through the example of the $K_0^*(727)$, how the light scalar mesons can be described by S-matrix singularities which are not directly related to the ground states of the $J^P = 0^+$ confinement spectrum.

The RSE parameters $B_{n\ell_c}$ of formula (12) incorporate the unknowns of hadronic decay processes. Empirical knowledge of these parameters will certainly give a substantial contribution to the detailed study of hadronic decay at low and intermediate energies.

With respect to the quantitative conclusions of the present work, a word of caution is in place. Since expression (8) allows for it, we may also inspect the effects of higher thresholds. This has been carried out for harmonic-oscillator confinement in the model of [10–15], with the following results: for P-wave non-exotic two-meson scattering, both with $J^{PC} = 0^{-+}$ and $J^{PC} = 1^{--}$, the real parts of the singularities which correspond to the ground states at $E_{0,0}$ of the confinement spectrum come out some 300–400 MeV below $E_{0,0}$. For the higher radial excitations these shifts are considerably smaller. For S-waves the shifts are also smaller for the ground states and, moreover, in the positive direction. When we compare these findings with the one-threshold results shown above, we must conclude that higher thresholds should be taken into account for a more quantitative determination of the confinement and decay mechanisms. In particular, the second singularity of formula (22) might come out rather displaced, if higher thresholds are accounted for. This will be investigated in future work.

Acknowledgements. We are indebted to Jeffrey Appel for drawing our attention to the need for a more phenomenological ap-

proach to data analysis in coupled-channel models for confinement and hadronic decay. We also wish to thank Alexander A. Osipov, Brigitte Hiller, Alex Blin and Hans Walliser for useful discussions and suggestions. This work is partly supported by the Fundação para a Ciência e a Tecnologia under contract numbers PESO/P/PRO/15127/99, POCTI/35304/-FIS/2000 and CERN/P/FIS/40119/2000.

References

1. F. Butler, H. Chen, J. Sexton, A. Vaccarino, D. Weingarten, Nucl. Phys. B **430**, 179 (1994) [hep-lat/9405003]
2. D. Weingarten, Nucl. Phys. B **215**, 1 (1983)
3. H. Hamber, E. Marinari, G. Parisi, C. Rebbi, Phys. Lett. B **108**, 314 (1982)
4. H. Hamber, G. Parisi, Phys. Rev. Lett. **47**, 1792 (1981)
5. E. van Beveren, C. Dullemond, T.A. Rijken, Z. Phys. C **19**, 275 (1983)
6. A.A. Khan et al. [CP-PACS Collaboration], hep-lat/0105015
7. S. Aoki et al. [CP-PACS Collaboration], Phys. Rev. Lett. **84**, 238 (2000) [hep-lat/9904012]
8. Yoshinobu Kuramashi for the CP-PACS Collaboration, Proceedings of the Meeting of Particles and Fields of the American Physical Society (DPF99), Los Angeles, CA, 5–9 January 1999 [hep-lat/9904003]
9. W. Lee, D. Weingarten, Phys. Rev. D **61**, 014015 (2000) [hep-lat/9910008]; hep-lat/9805029; Nucl. Phys. Proc. Suppl. **53**, 236 (1997) [hep-lat/9608071];
   D. Weingarten, private communication
10. E. van Beveren, T.A. Rijken, K. Metzger, C. Dullemond, G. Rupp, J.E. Ribeiro, Z. Phys. C **30**, 615 (1986)
11. E. van Beveren, G. Rupp, T.A. Rijken, C. Dullemond, Phys. Rev. D **27**, 1527 (1983)
12. C. Dullemond, G. Rupp, T.A. Rijken, E. van Beveren, Comp. Phys. Comm. **27**, 377 (1982)
13. E. van Beveren, C. Dullemond, G. Rupp, Phys. Rev. D **21**, 772 (1980); Erratum ibid. D **22**, 787 (1980)
14. E. van Beveren, Z. Phys. C **21**, 291 (1984)
15. E. van Beveren, G. Rupp, Phys. Lett. B **454**, 165 (1999) [hep-ph/9902301]
16. K. Abe et al. [SLD Collaboration], Phys. Rev. D **59**, 012002 (1999) [hep-ex/9805023]
17. E. van Beveren, Zeit. Phys. C **17**, 135 (1983)
18. E. van Beveren, G. Rupp, Eur. Phys. J. C **11**, 717 (1999) [hep-ph/9806248]
19. Joannis Papavassiliou, hep-ph/0102149
20. V.K.B. Kota, R. Sahu, nucl-th/0006079
21. Ron Workman, Phys. Rev. C **59**, 3441 (1999) [nucl-th/9811056]; nucl-th/0104028
22. M. Moshinsky, Proceedings of the International Conference on Hadron Spectroscopy, Hadron 91, College Park, MD, 12–16 August 1991, pp. 342–355
23. Yu-Bing Dong, Phys. Lett. B **418**, 355 (1998)
24. Z.Y. Fang, G. Lopez Castro, J. Pestieau, Nuovo Cim. A **100**, 155 (1988)
25. V.M. Weinberg, ITEP-160-1982 (Moscow, ITEP 1982)
26. Marius Orlowski, Nuovo Cim. A **80**, 89 (1984)
27. P. Estabrooks, R.K. Carnegie, A.D. Martin, W.M. Dunwoodie, T.A. Lasinski, D.W. Leith, Nucl. Phys. B **133**, 490 (1978)
28. O. Dumbrajs, R. Koch, H. Pilkuhn, G.C. Oades, H. Behrens, J.J. De Swart, P. Kroll, Nucl. Phys. B **216**, 277 (1983)
29. C.B. Lang, Nuovo Cim. A **41**, 73 (1977)
30. N. Johannesson, G. Nilsson, Nuovo Cim. A **43**, 376 (1978)
31. A. Karabarbounis, G. Shaw, J. Phys. G **6**, 583 (1980)
32. V. Bernard, N. Kaiser, U.G. Meissner, Phys. Rev. D **43**, 2757 (1991)
33. P. Estabrooks, Phys. Rev. D **19**, 2678 (1979)
34. D. Aston et al., Nucl. Phys. B **296**, 493 (1988)
35. M.J. Matison et al., Phys. Rev. D **9**, 1872 (1974)
36. Carla Göbel, on behalf of the E791 Collaboration, hep-ex/0012009
37. Deidre Black, Amir H. Fariborz, Sherif Moussa, Salah Nasri, Joseph Schechter, Phys. Rev. D **64**, 014031 (2001) [hep-ph/0012278]
38. Deirdre Black, Amir H. Fariborz, Joseph Schechter, Proceedings of the YITP Workshop on Possible Existence of the Sigma Meson and its Implications to Hadron Physics, Sigma Meson 2000, Kyoto, Japan, 12–14 June 2000 [hep-ph/0008246]; Proceedings of the International Workshop on Hadron Physics: Effective Theories of Low Energy QCD, Coimbra, Portugal, 10–15 September 1999, AIP Conference Proceedings **508**, 290–299 (2000) [hep-ph/9911387]; Phys. Rev. D **61**, 074001 (2000) [hep-ph/9907516]
39. M.D. Scadron, Proceedings of the YITP Workshop on Possible Existence of the Sigma Meson and its Implications to Hadron Physics, Sigma Meson 2000, Kyoto, Japan, 12–14 June 2000 [hep-ph/0007184]
40. Matthias Jamin, Jose Antonio Oller, Antonio Pich, Nucl. Phys. B **587**, 331 (2000) [hep-ph/0006045]
41. Shin Ishida, Muneyuki Ishida, Tomohito Maeda, Prog. Theor. Phys. **104**, 785 (2000) [hep-ph/0005190]
42. L. Babukhadia, Ya.A. Berdnikov, A.N. Ivanov, M.D. Scadron, Phys. Rev. D **62**, 037901 (2000) [hep-ph/9911284]
43. V.E. Markushin, M.P. Locher, Proceedings of the Workshop on Hadron Spectroscopy (WHS 99), Rome, Italy, 8–12 March 1999, Frascati 1999, Hadron Spectroscopy, pp. 229–236 (1999) [hep-ph/9906249]
44. J.L. Lucio Martinez, Mendivil Napsuciale, Phys. Lett. B **454**, 365 (1999) [hep-ph/9903234]
45. Muneyuki Ishida, Prog. Theor. Phys. **101**, 661 (1999) [hep-ph/9902260]
46. Amir H. Fariborz, Joseph Schechter, Phys. Rev. D **60**, 034002 (1999) [hep-ph/9902238]
47. Deirdre Black, Amir H. Fariborz, Francesco Sannino, Joseph Schechter, Phys. Rev. D **59**, 074026 (1999) [hep-ph/9808415]; Phys. Rev. D **58**, 054012 (1998) [hep-ph/9804273]
48. J.A. Oller, E. Oset, Phys. Rev. D **60**, 074023 (1999) [hep-ph/9809337]
49. J.A. Oller, E. Oset, J.R. Pelaez, Phys. Rev. D **59**, 074001 (1999); Erratum ibid. D **60**, 099906 (1999) [hep-ph/9804209]; Phys. Rev. Lett. **80**, 3452 (1998) [hep-ph/9803242]
50. Shin Ishida, Muneyuki Ishida, Taku Ishida, Kunio Takamatsu, Tsuneaki Tsuru, Prog. Theor. Phys. **98**, 621 (1997) [hep-ph/9705437]
51. V.V. Anisovich, Phys. Usp. **41**, 419 (1998) [Usp. Fiz. Nauk **168**, 481 (1998)] [hep-ph/9712504]

52. M. Koll, R. Ricken, D. Merten, B.C. Metsch, H.R. Petry, Eur. Phys. J. A **9**, 73 (2000) [hep-ph/0008220]
53. R.F. Dashen, J.B. Healy, I.J. Muzinich, Phys. Rev. D **14**, 2773 (1976); Ann. Phys. **102**, 1 (1976)
54. J. Weinstein, Nucl. Phys. Proc. Suppl. **21**, 207 (1991); UTK-89-7, Invited talk given at Hadron '89, International Conference on Hadron Spectroscopy, Ajaccio, France, 23–27 September 1989; UTK-HEP-TH-88-49, Presented at BNL Workshop on Glueballs, Hybrids, and Exotic Hadrons, Upton, N.Y., 29 August–1 September 1988
55. J. Weinstein, N. Isgur, Phys. Rev. D **43**, 95 (1991); Phys. Rev. D **41**, 2236 (1990)